Raman spectroscopy of Cs_2HgBr_4 at high pressure: effect of hydrostaticity

2006 J. Phys.: Condens. Matter 18 3443

(http://iopscience.iop.org/0953-8984/18/13/012)

INSTITUTE OF PHYSICS PUBLISHING JOURNAL OF PHYSICS: CONDENSED MATTER

J. Phys.: Condens. Matter **18** (2006) 3443–3453 doi:10.1088/0953-8984/18/13/012

Raman spectroscopy of Cs_2HgBr_4 at high pressure: effect of hydrostaticity

D Machon[1,2], P Bouvier[2], P Tolédano[3] and H-P Weber[4,5]

[1] LPMCN, Université Lyon-I, Bâtiment Léon Brillouin, 43 boulevard du 11 Novembre 1918, F-69622 Villeurbanne cedex, France
[2] LEPMI, INPG-CNRS, 1130 rue de la piscine, BP75 38402 St Martin d'Hères Cedex, France
[3] Department of Physics, University of Picardie, 33 rue Saint-Leu, 80000 Amiens, France
[4] LCr/IPMC/FSB, Swiss Federal Institute of Technology, CH-1015 Lausanne, Switzerland
[5] ACCE, Grand Vivier, F-38960 St Aupre, France

Received 9 December 2005, in final form 21 February 2006
Published 14 March 2006
Online at stacks.iop.org/JPhysCM/18/3443

Abstract

Raman spectra have been measured on Cs_2HgBr_4 as a function of pressure, degree of hydrostaticity and location in the sample chamber. In the absence of a pressure-transmitting medium the title compound transforms reversibly into an amorphous phase at about 9 GPa, and this throughout the sample chamber. When argon is used as pressure-transmitting medium in a similar pressure range, different areas (with an approximate radius of 2 μm) of the pressure chamber yield dissimilar Raman spectra, varying from complete amorphization to a crystal-to-crystal transition. The results from this Raman study are combined with previous x-ray diffraction results and simulations on the same compound to give a comprehensive picture of the formation of a ferroelastic glass state.

1. Introduction

The first generally accepted occurrence of pressure-induced amorphization (PIA) was reported in 1984 in hexagonal ice, from quenched samples [1]. The first *in situ* evidence of a crystalline-to-amorphous (c–a) phase transition under pressure was discovered in SnI_4 from laboratory x-ray diffraction data and from Raman measurements, both in 1985 [2, 3]. The discovery of this new effect immediately triggered a wide-ranging search for similar phases in other chemical systems [4, 5]. While the first materials had been obtained solely on compression of an initially crystalline material, amorphous materials were later also obtained from decompression of an initially crystalline material synthesized at high pressure [5, 6]. By the early 1990s a large number of compounds were reported to become amorphous under pressure; the phenomenon seemed to be common-place, and, as a result, interest in PIA waned, even though in many cases the c–a mechanism remained unexplained. In the late 1990s, with the advent of more powerful experimental techniques such as the combination of synchrotron radiation, diamond-anvil cell and area detector, a closer look at some reportedly

key compounds such as quartz [7] and berlinite ($AlPO_4$) [8] suddenly failed to reveal an amorphous phase, in particular if the incident x-ray beam was small enough to avoid sample regions with pressure gradients or if hydrostaticity was assured by the use of an appropriate pressure medium. As a result, the field of PIA studies became now wide open again, and ripe for another experimental assault, at an increased level of technical sophistication, as compared to the past.

In the early days of this burgeoning field, due to the less than optimal quality of the data, speculations as to the forces driving the effect abounded. Solely, apparent loss of long-range order seemed to be the common characteristic. Until recently one distinguished mainly between two mechanisms:

(a) decomposition of an initially structurally complex crystal into simpler components,
(b) kinetically impeded transition between crystalline states being able to induce genuine structural disorder on the atomic scale.

In a recent paper [9], the concept of a ferroelastic glass state was proposed by the authors of the present work. This model is the mechanical analogue of dipole or spin glasses. In some sense, it is an extension of the second mechanism mentioned above, but it provides a more consistent interpretation of past and present experimental observations of PIA. The conditions to obtain a ferroelastic glass are developed in [9]. For the present purpose, we summarize the model and conditions as follows. If we apply to a material close to a ferroelastic transition a non-hydrostatic compression corresponding to a stress-field tensor involving shear stresses, it may either produce a crystalline phase with a stable crystalline configuration or cause the formation of a 'frustrated' multi-domain state, in which the different crystalline domains induced by the stress-field tensor occur simultaneously. Structural mismatches between adjacent differently sheared domains then give rise to internal stresses that produce a splitting of the mesoscopically sized domains and their progressive disintegration into ferroelastic nanodomains that appear at the length scale of x-ray diffraction experiments as a *glassy state*. Such a ferroelastic glass may form instead of its crystalline counterpart if

(a) the ferroelastic phase exists in equivalent configurations corresponding to distinct spontaneous strain components, and
(b) an internal stress-field is created in the sample which includes the stress components conjugated to the spontaneous strains.

In the following the terms amorphous/amorphization solely imply an *apparent* loss of long range order as observed in Raman or x-ray diffraction patterns. Whether full structural randomization has occurred on an atomic scale cannot be inferred from these types of observations.

Earlier studies on Cs_2HgBr_4 at ambient pressure [10, 11] have disclosed, on cooling, the following sequence of phases below the parent room-temperature orthorhombic phase (space-group $Pnma$, $Z = 4$): an incommensurate phase occurring below $T_i = 243$ K, with a modulation wavevector $\mathbf{k}_i = 0.15\mathbf{a}^*$, followed by a ferroelastic phase of monoclinic symmetry ($P2_1/n$, $Z = 4$) at the lock-in transition temperature $T_c = 230$ K and lock-in vector $\mathbf{k}_c = 0$, and by a triclinic ferroelastic phase ($P\bar{1}$, $Z = 4$) at $T_1 = 165$ K, with $\mathbf{k}_1 = 0$. The monoclinic phase gives rise to a pair of sheared domains with the spontaneous strains $\pm e_{xy}$ whereas an additional pair of domains, involving the shear strains e_{xz} and e_{yz}, appears in the triclinic phase. According to the conditions required for the formation of a ferroelastic glass (see [9]), ferroelastic phases can be realized in differently strained configurations corresponding to the same point-group symmetries. Their existence then suggests that, under the condition where

the stability of these phases persists up to high pressures in the phase diagram of Cs_2HgBr_4, one should be able to obtain a ferroelastic glass state by applying to this material a non-hydrostatic pressure that would induce an internal shear stress-field in the sample.

The preceding model was substantiated by x-ray diffraction studies on Cs_2HgBr_4 [12], showing the following.

(1) In the absence of any pressure-transmitting medium (PTM), the diffraction peaks broaden above 11 GPa merge into haloes typical of amorphous solids. The halo pattern is fully achieved at 18 GPa and remains unchanged up to 37.2 GPa. On decompression the halo persists down to 1 GPa, and the orthorhombic structure is restored at ambient pressure.
(2) With paraffin oil as the PTM a single halo is obtained from 14 GPa upward.
(3) With nitrogen as the PTM the diffraction patterns show crystalline features up to 31 GPa, and no amorphization is observed. While paraffin is expected to provide quasi-hydrostatic conditions up to 8 GPa, nitrogen is known to ensure even better quasi-hydrostatic conditions up to 16.5 GPa (corresponding to the onset of the harder ε-N_2 phase).
(4) The same experiment performed on a single crystal of Cs_2HgBr_4, using paraffin oil as the PTM, shows no broadening of the peaks up to 13 GPa, but a sequence of two phase transitions, similar to the sequence reported at ambient pressure below 243 K: an incommensurate phase arising at 1.2 GPa, followed at 10.3 GPa by a lock-in monoclinic phase with the space group $P2_1/n$ ($Z = 4$).

In this work, we present Raman studies of Cs_2HgBr_4 powder under different compression conditions. These studies confirm the x-ray observations but show that the spectral information varies drastically as a function of the sample area probed. This is interpreted as a further support for an interpretation in terms of the formation of a ferroelastic glass state.

2. Experimental details

Raman spectra of Cs_2HgBr_4 powder were recorded in back-scattering geometry with a confocal T64000 multi-channel spectrometer equipped with a CCD detector. The 514.5 nm line from an Argon ion laser was used as the excitation source, with the light focused on the sample through the 20× objective of a microscope such that the irradiated diameter was about 2 μm. Recording spectra at different incident powers checked for heating of the sample by the laser beam. An incident power of 15 mW was found to be appropriate for the present study. High-pressure experiments were performed in a membrane diamond-anvil cell. The powdered sample was loaded into a chamber 125 μm in diameter and 30 μm thick drilled in a stainless steel gasket. Two experiments were carried out. During the first one, the sample was loaded in the cell without a PTM to provide non-hydrostatic compression. During the second one, the PTM argon was cryogenically loaded as a fluid into the cell, and used as a nearly hydrostatic medium during pressurization experiments. The pressure was monitored with a ruby chip placed in the vicinity of the sample [13]. Hydrostaticity was inferred from the width of the Cr^{3+} fluorescence lines of the ruby.

3. Structure and Raman-active modes

The ionic compounds with generic formula A_2BX_4 are made of cations A and anionic tetrahedra BX_4. The orthorhombic structure stable at room conditions is described by the space group $Pnma$ (D_{2h}^{16}). The cell parameters for Cs_2HgBr_4 are $a_o = 10.248$ Å, $b_o = 7.927$ Å and $c_o = 13.901$ Å [14]. This structure may also be described by a pseudo-hexagonal cell with the

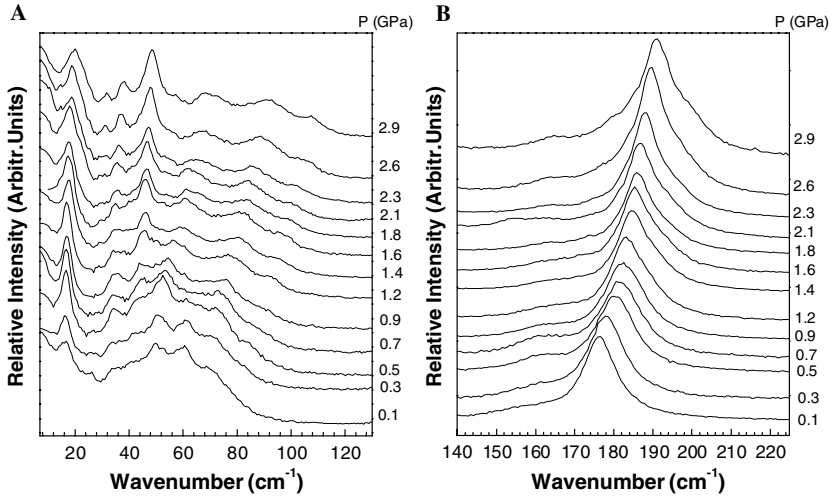

Figure 1. Evolution of Cs_2HgBr_4 Raman spectra with applied pressure between 0.1 and 2.9 GPa. (A) Lattice modes and bending internal modes; (B) stretching internal modes. This run was performed without any pressure-transmitting medium.

a-axis being the six-fold axis. This is supported by the c_o/b_o ratio being equal to 1.754 close to $\sqrt{3}$, as expected for an ideal hexagonal structure.

In phonon spectra of Cs_2HgBr_4, the 28 atoms in the unit cell of the orthorhombic structure give rise to 81 ($\mathbf{k} = 0$) optical modes that can be characterized according to the space group using a group-theoretical method. Such a treatment leads to 42 Raman-active modes,

$$\Gamma_{\text{raman}} = 13A_g + 8B_{1g} + 13B_{2g} + 8B_{3g}.$$

4. Results

4.1. Measurements without any pressure-transmitting medium: non-hydrostatic conditions

A transition to an incommensurate phase has been observed previously by x-ray diffraction at 1.2 GPa [12]. In the present Raman spectra, recorded in the absence of a PTM, this phase transition is observed as well (figure 1), mainly in the low-frequency range. The line at 60 cm^{-1} disappears around 1.0 GPa while the lines at 25 and 45 cm^{-1} appear above 2.3 and 1.2 GPa, respectively, increasing in strength with pressure. One can also observed a change in the stretching modes (160–200 cm^{-1}) with the appearance of an asymmetry on the high-frequency side between 0.9 and 1.2 GPa. This feature increases at higher pressure. With increasing pressure, in the pressure range 3.0–14.0 GPa, but especially above 8.4 GPa, we observed (figure 2) a gradual disappearance of the lattice modes ($\sim$10–125 cm^{-1}) as well as a progressive broadening of the lines associated with the internal vibration modes ($\sim$150–250 cm^{-1}).

We conclude that in this material, PIA under non-hydrostatic pressure starts around 9.0 GPa and is completed by about 12.0 GPa, in good agreement with our previous x-ray diffraction observations [12]. Different areas of the sample were analysed in the diamond-anvil cell; they all display the same amorphous spectrum. Therefore the transformation takes place in a homogeneous fashion throughout the whole sample chamber.

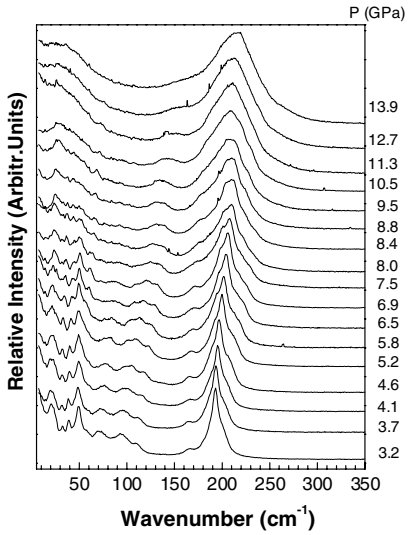

Figure 2. Evolution of Cs_2HgBr_4 Raman spectra with applied pressure between 3.2 and 13.9 GPa. This run was performed without any pressure-transmitting medium.

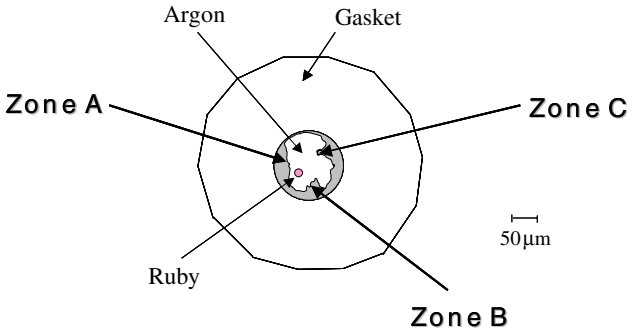

Figure 3. Schematic representation of the sample chamber during the second run using argon as the pressure-transmitting medium. The grey part represents the sample.

(This figure is in colour only in the electronic version)

4.2. Measurements with argon as the pressure-transmitting medium: quasi-hydrostatic conditions

The initial pressure was 3.9 GPa, resulting from the need to seal the argon in the diamond-anvil cell under pressure (for this reason we could not obtain any information regarding the first phase transition at lower pressure). Figure 3 shows the spatial relationships amongst different regions of the load in the diamond-anvil gasket hole. During this experiment three different zones of the load were probed in the diamond anvil cell (referred to as A (figure 4), B (figure 5) and C (figure 6) in figure 3).

The crucial advantage of the Raman spectroscopy technique, as compared to routine x-ray diffraction, is that it allows the analysis of very small sample areas, of the order of 2 μm. This adds substantially to the information already derived previously from x-ray diffraction.

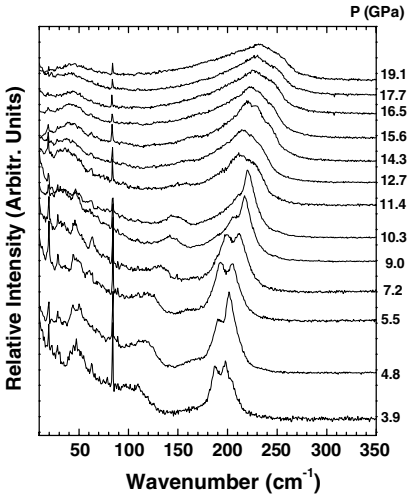

Figure 4. Evolution of Cs_2HgBr_4 Raman spectra with applied pressure between 3.9 and 19.1 GPa in zone A. This run was performed with argon as the pressure-transmitting medium. The line at 75 cm^{-1} is a plasma line from the laser.

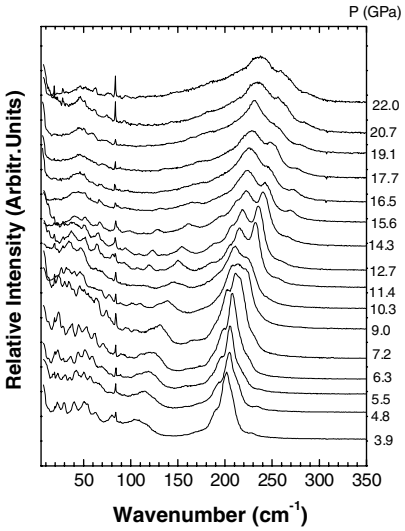

Figure 5. Evolution of Cs_2HgBr_4 Raman spectra with applied pressure between 3.9 and 22.0 GPa in zone B. This run was performed with argon as the pressure-transmitting medium. The line at 75 cm^{-1} is a plasma line from the laser.

Zone A. Raman spectra recorded with increasing pressure are shown in figure 4. At 3.9 GPa, a well-resolved splitting is observed in the two components around 180–200 cm^{-1}. Polarization as a cause could be discounted, as changing the polarization did not lead to any noticeable change in the spectrum.

Under non-hydrostatic compression (see section 4.1), this splitting was not observed as clearly. However, a similar behaviour is noticeable at pressures higher than 5.8 GPa (figure 2). Above 9.0 GPa the intensity of the split lines at $\sim$210 cm^{-1} decreases. Above 11.4 GPa

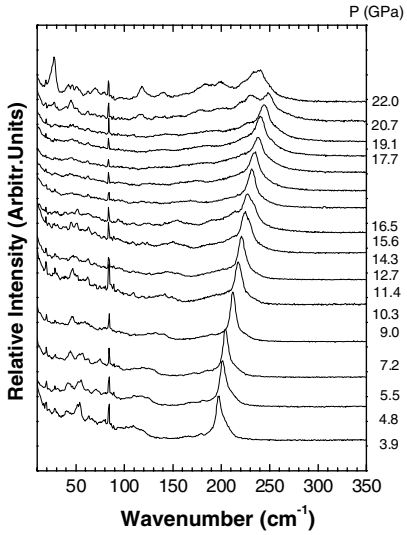

Figure 6. Evolution of Cs_2HgBr_4 Raman spectra with applied pressure between 3.9 and 22.0 GPa in zone C. This run was performed with argon as the pressure-transmitting medium. The line at 75 cm^{-1} is a plasma line from the laser.

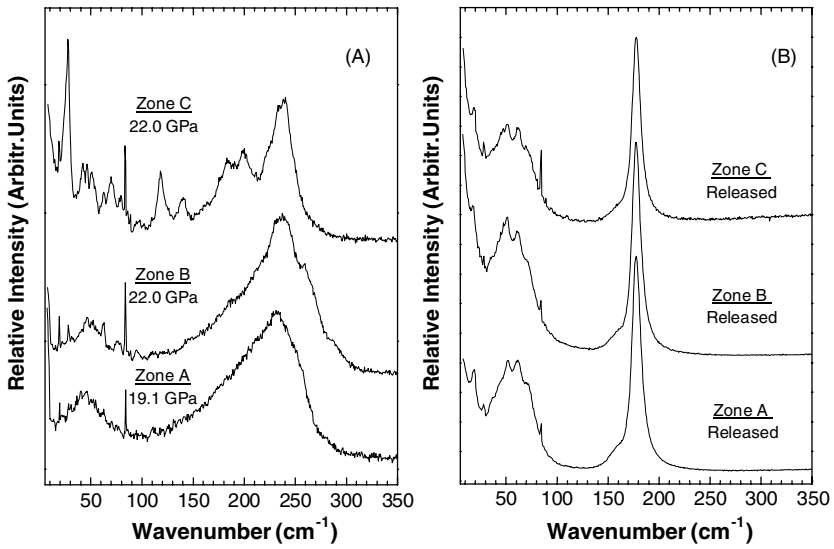

Figure 7. Comparison of Cs_2HgBr_4 Raman spectra obtained in the zones A, B, and C defined in figure 3. (A) Spectra recorded at the highest pressure. (B) Spectra recorded after decompression. The line at 75 cm^{-1} is a plasma line from the laser.

an important broadening of both high-frequency and low-frequency modes takes place, in particular those lines associated with the bending internal modes (100 cm^{-1}). Some lattice modes around 15 cm^{-1} are still observed up to 15–16 GPa.

At ambient pressure, the spectrum expected for the initial *Pnma* structure is recovered (figure 7). In summary, we conclude that a transition to an amorphous phase occurs progressively between 11.4 and 16.5 GPa, and that, most importantly, this transition is fully

reversible when the pressure is released (figure 7). The appearance of an amorphous-like pattern was also observed by x-ray diffraction [12] in the pressure range of the phase transition from the incommensurate to the lock-in phase.

Zone B. Spectra recorded with increasing pressure are presented in figure 5. The spectral evolution in this zone is similar to the one observed in zone A but with a 7 GPa shift. The splitting of the peaks at 180–200 cm^{-1} starts at 11.4 and disappears above 16.5 GPa. It is worth noting that this splitting appears at the lock-in transition observed previously in single-crystalline Cs_2HgBr_4 [12]. Above 14 GPa, the low-frequency modes also disappear, and above 19 GPa, the high-frequency lines broaden drastically. At 22 GPa, a structure in the 200–300 cm^{-1} band is still observable but one can conclude that the amorphization process is in its last stage. In that zone, we also observed under decompression a complete reversibility to the initial spectrum (figure 7).

Zone C. Figure 6 shows the spectra obtained with increasing pressure. The key observation here is that the spectra from this region of the load do not reveal any amorphization. Until the pressure reaches 20.7 GPa no splitting of the high-frequency lines is observed. In the pressure range 14.0–19.0 GPa the lattice modes are hardly observable. However, at higher pressure, between 20.0 and 22.0 GPa, the Raman spectra show unambiguously a structural change. The appearance of new peaks in the whole frequency range, and especially the strong line around 30 cm^{-1}, indicates a crystal–crystal phase transition.

As in regions A and B, all of these changes are also completely reversible, and the initial spectrum is recovered upon decompression (figure 7). In summary, the fact that Raman spectroscopy allows one to probe small, selected areas of a pressurized sample, and to study their evolution with pressure, provides us with a very sensitive probe of *hydrostaticity*.

In the non-hydrostatic compression regime, between 8.0 and 10.0 GPa, amorphous-*like* spectra appear homogeneously throughout the sample. Inhomogeneity in sample behaviour is observed when argon is used as the PTM. Our previous x-ray study [12] did not permit a sampling small enough to detect such deviation from homogeneity, and figure 5(c) of [12] shows an average over most of the whole sample chamber. Figure 7 summarizes the observation obtained. At 22.0 GPa, in zones A, B and C, we observed, respectively, a total amorphization, a partial amorphization and a new crystal polymorph. However, after decompression, all spectra are identical, and correspond to the initial crystalline *Pnma* phase. The question to be answered now is: What is the mechanism driving the amorphization?

5. Discussion

The present work, in addition to the previous x-ray diffraction study [12], shows that the high-pressure behaviour of Cs_2HgBr_4 is extremely sensitive to deviations from ideal hydrostaticity. The notion of hydrostaticity is itself qualitative and relative, i.e., depending on the mechanical properties of the compressed sample with regard to the PTM ones. A liquid is considered as the best PTM. However, pressure will favour solidification, and the softer solidified PTM will provide the better quasi-hydrostatic conditions. In the pressure range 0.1–15.0 GPa, nitrogen and argon are the most used PTMs because they remain soft although in their solid form, and they are easy to load in a diamond-anvil cell. A tentative estimate of the degree of hydrostaticity was obtained by monitoring the ruby luminescence line width with increasing pressure [15]. In figure 8, one can see this width evolution for the two experiments presented here (without any PTM and with argon as the PTM). The loss of hydrostaticity when no PTM is used takes place

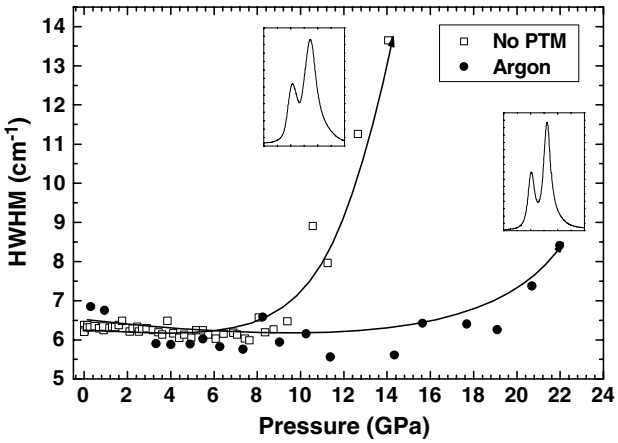

Figure 8. Half-width at half maximum (HWHM) evolution of the luminescence ruby line in both experiments. Open squares: without any pressure-transmitting medium; circles: argon as the PTM. The lines are guides to the eyes. The two insets show the ruby fluorescence lines at 13.9 GPa during the non-hydrostatic run (no PTM) and at 22.0 during the quasi-hydrostatic run (Ar as the PTM).

at a pressure lower than when argon is used as the PTM. In the non-hydrostatic run, the loss of hydrostaticity occurs at 10–12 GPa. In the quasi-hydrostatic run, it is difficult to infer a loss of hydrostaticity from the ruby line.

However, this method only determines the local hydrostaticity experienced by the ruby chip. The hydrostaticity experienced by the sample itself is more difficult to extract. The form (powder versus single crystal) of the sample is then crucial, as shown in [12]. Using an identical PTM, a large Cs_2HgBr_4 single crystal shows x-ray diffraction at 13 GPa while a powdered sample shows an amorphous-like diffraction pattern at the same pressure. Compression, even highly hydrostatic, of a powdered sample will give rise to *localized shear stresses* because of intergranular contacts. These can only be avoided if all the single-crystals grains constituting the sample are surrounding by the PTM. This ideal situation is difficult to control, and is, in practice, impossible to achieve.

Therefore, the nature of the compression (hydrostatic versus non-hydrostatic) experienced locally by the sample can only be inferred by its own response to the structural characterization probe, Raman spectroscopy in our case. In the set of experiments with argon as the PTM, two main features of the spectra differentiate the zones: a splitting of the high-frequency modes and the appearance of an amorphous-like spectrum at higher pressure. An important question that arises is whether or not there is any correlation between these two behaviours. One can argue that shear stresses induce local distortion giving rise to this splitting. However, this effect is only qualitative and, moreover, the structure is incommensurate between 1.2 and 11.7 GPa according to x-ray experiment [12]. Therefore, one cannot infer any direct correlation between the splitting and the amorphous-like spectrum at that stage. Still, it is worth noting that such a splitting is also observed when no PTM is used at pressure higher than 8.0 GPa. In this case, this effect is less marked because the stresses are highly inhomogeneous, and lead to a broadening of the Raman lines that, eventually, would mask the splitting.

The second difference between the spectra in the zones A, B and C is the appearance of an amorphous-like spectrum. This kind of spectrum is also observed in the whole sample chamber during the non-hydrostatic compression. In addition, this amorphization disappears when stresses are released whatever the compression conditions are. These observations

suggest a mechanical mechanism. However, if the existence of non-hydrostatic stresses is a necessary condition to observe PIA, it is not sufficient, otherwise PIA would be a more common observation during high-pressure experiments. The observation of PIA in some compounds, and particularly in Cs_2HgBr_4, can be explained on the basis of the ferroelastic glass model developed in [9]. In this model the combination of non-hydrostatic stresses and the occurrence of a ferroelastic phase transition leading to the appearance of internal shear stresses at the paraelastic-to-ferroelastic transition is the key factor to obtain a ferroelastic glass. In this state, x-ray diffraction patterns and Raman spectra are similar to those of an amorphous compound. In our previous study [12], we have shown that, under quasi-hydrostatic conditions, the amorphous phase is replaced by a crystalline phase of point symmetry $2/m$. There is a group to subgroup relationships between this phase and the low-pressure parent phase *mmm*. The symmetry change $mmm \rightarrow 2/m$ corresponds to a paraelastic-to-ferroelastic transition. Three monoclinic non-equivalent configurations are obtained: $2_x/m_x$, $2_y/m_y$ and $2_z/m_z$ with distinct strains (e_{yz}, e_{xz} and e_{xy}, respectively). Each configuration gives rise to two energetically equivalent ferroelastic domains transforming into one another by the symmetry operations lost at the transition. Applying to the material close to this ferroelastic transition a non-hydrostatic compression corresponding to a stress-field tensor involving the shear stresses e_{yz}, e_{xz} and e_{xy} will either produce a crystalline phase with a stable monoclinic configuration or result in the formation of a 'frustrated' multi-domain state, in which the six monoclinic domains induced by the stress-field tensor take place simultaneously.

Moreover, at the *proper* ferroelastic phase transition occurring in Cs_2HgBr_4, the magnitude of the deformation will be strongly dependent on the conjugated stress-field. Therefore, an inhomogeneous stress-field will give rise to a highly inhomogeneous deformation field. This argument is strongly supported by our numerical simulations of the diffraction patterns in [12]. In this work, the evolution of the diffraction patterns with pressure, including the appearance of an amorphous-like halo, was reproduced using a Gaussian distribution of the deformations. The existence of an inhomogeneous deformation assumed in [12] for the interpretation of the diffraction patterns is therefore consistent with the mechanism underlying the formation of a ferroelastic glass state [9].

6. Summary and conclusion

High-pressure Raman spectroscopy experiments have been performed on Cs_2HgBr_4, while varying the degree of hydrostaticity. During non-hydrostatic compression, at pressures below 12 GPa, the Raman spectra throughout the sample chamber are typical of amorphous compounds. When using instead argon as the PTM, i.e., with the sample powder under hydrostatic conditions, the Raman spectra differed from one part of the sample chamber to the next. For the three points measured we observe a complete crystal-to-amorphous transition, a partial crystal-to-amorphous transitions or a crystal-to-crystal transition. On the other hand, the amorphization process is favoured when the samples are in powder form, and shear stress-fields are present due to non- or partial hydrostaticity. When the samples are either a powder or a single crystal but embedded in a good hydrostatic PTM, a transition to a crystalline ferroelastic is preferred over amorphization. A characteristic common to all the observed PIA phases is that they revert to their crystalline counterparts, once the pressure is released.

A unifying interpretation of the preceding facts can be proposed if one assumes that non-hydrostatic compression induces a shear stress-field which triggers the onset of a ferroelastic glass state formed by differently shear-strained nanodomains. This process is expected to occur more favourably in powder samples, as grain to grain contacts give rise to large deviatoric stresses which enhance the splitting of the ferroelastic domains. The inhomogeneous (three-

region) amorphization observed in the Raman experiments confirms the sensitivity of *the amorphization mechanism to the internal stress-field existing in the diamond anvil-cell* and to its localized character: small stress-field variations may preserve the crystallinity in localized regions of the sample or on the contrary trigger the amorphization mechanism.

Acknowledgments

We thank Dr Julian Haines (Laboratoire de Physico-Chimie de la Matière Condensée, Université Montpellier II) for his comments. One of us (HPW) wishes to acknowledge the steadfast financial support of the Swiss National Science Foundation throughout his work on pressure-induced amorphization.

References

[1] Mishima O, Calvert L D and Whalley E 1984 *Nature* **310** 393
[2] Fuji Y, Kowaka M and Onodera A 1985 *J. Phys. C: Solid State Phys.* **18** 789
[3] Sugai S 1985 *J. Phys. C: Solid State Phys.* **18** 799
[4] Richet P and Gillet P 1997 *Eur. J. Mineral.* **9** 907
[5] Sharma S M and Sikka S K 1996 *Prog. Mater. Sci.* **40** 1
[6] Richet P 1988 *Nature* **331** 56
[7] Haines J, Léger J M, Gorelli F and Hanfland M 2001 *Phys. Rev. Lett.* **87** 155503
[8] Sharma S M, Garg N and Sikka S K 2000 *Phys. Rev.* B **62** 8824
[9] Tolédano P and Machon D 2005 *Phys. Rev.* B **71** 024210
[10] Pinheiro C B, Jorio A, Pimenta M A and Speziali N L 1998 *Acta Crystallogr.* B **54** 197
[11] Kityk A V, Zadorozhna A V, Schur Ya I, Martin-Lotoska I Yu, Burak Ya and Vlokh O G 1998 *Aust. J. Phys.* **51** 943
[12] Machon D, Dmitriev V P, Bouvier P, Timonin P N, Shirokov V B and Weber H-P 2003 *Phys. Rev.* B **68** 144104
[13] Mao H K, Bell P M, Shaner J W and Steinberg D J 1978 *J. Appl. Phys.* **49** 3276
[14] Jorio A, Dantas M S S, Pinheiro C B, Speziali N L and Pimenta M A 1998 *Phys. Rev.* B **57** 203
[15] Bouvier P and Lucazeau G 2000 *J. Phys. Chem. Solids* **61** 569